Journal of Applied Fluid Mechanics, Vol. 13, No. 1, pp. 161-168, 2020.
Available online at www.jafmonline.net, ISSN 1735-3572, EISSN 1735-3645.
DOI: 10.29252/jafm.13.01.30350

CFD-DEM Simulation to Predict the Critical Velocity of Slurry Flows

J. R. Januário and C. B. Maia†

Pontifical Catholic University of Minas Gerais, Dom José Gaspar Avenue, 500, Belo Horizonte, MG, 30535-901, Brazil

†*Corresponding Author Email: cristiana@pucminas.br*

(Received April 5, 2019; accepted June 7, 2019)

ABSTRACT

The hydraulic transport of solids has been adopted for many years. However, deposition of the solid particles in the pipe can cause equipment failure, pipeline erosion, and excessive pressure drop, resulting in financial and environmental problems. The critical velocity, also known as critical deposition velocity, is the limit of particle deposition when a moving bed of particles starts to form on the bottom of the pipe. The determination of the critical deposition velocity is an essential step in slurry pipeline`s design and operation. This paper assesses the influence of the velocity in the particle deposition of slurries containing coarse particles of apatite and hematite industrial concentrates and quartz. We used CFD to solve Navier-Stokes for the fluid phase and DEM to solve Newton`s equations governing the granular particles. CFD and the DEM modules adopted OpenFOAM and LIGGGHTS. Numerical results were compared with experimental data from the literature.

Keywords: CFD-DEM; Slurry flow; Critical deposition velocity; Numerical simulation.

NOMENCLATURE

C_μ	turbulence model constant	u	velocity
$C_{1\varepsilon}$	turbulence model constant		
$C_{2\varepsilon}$	turbulence model constant	ε	turbulent kinetic energy dissipation
E_{ij}	component of the deformation rate	σ_k	turbulence model constant
k	turbulent kinetic energy	σ_ε	turbulence model constant
p	pressure	ρ	specific mass
S	source term	μ_{eq}	dynamic equivalent viscosity
t	time	μ_t	turbulent viscosity

1. INTRODUCTION

Slurry pipeline transport is a commercially viable mode of transporting solid commodities as an alternative to truck and rail; nevertheless, it is a complex process (Vaezi, Verma and Kumar, 2018). The environmental and economic advantages of this method rather than by road or rail are being increasingly recognized by mining companies (Bhabra, 2013). The deposition of solid particles is one of the main difficulties faced when designing a slurry pipeline. The critical deposition velocity is the lower limit to operating velocities to avoid the formation of a bed at the bottom of the pipe. Operating above critical velocity is the best strategy to manage deposition and optimize production flow rates (Dabirian *et al.*, 2016). Nevertheless, it is difficult to accurately measure the critical velocity, because the critical condition is difficult to discern, and because the flow becomes unstable near the critical condition (Turian, Hsu and Ma, 1987).

Critical sand deposition velocities were experimentally determined by (Dabirian *et al.*, 2016), evaluating the effect of the sand concentration on the critical velocity. Six sand flow regimes were identified, and the authors concluded that particle size, particle concentration, and flow velocities have significant effects of the sand flow regimes. The viscosity effects on sand transport conditions and sand flow regimes were evaluated by (Zorgani *et al.*, 2018). The authors used visual observation and

camera to determine me sand transport velocity for water, CMC solutions, and oil, focusing on fluids with higher particle concentrations and carrier liquid viscosities lower than commonly found in oil pipelines. It was found that viscosity plays an important role in the sand minimum transport condition. A new experimental technique to measure deposition velocities in pipeline transport of solids was proposed by (Vaezi, Verma and Kumar, 2018). The authors used high-frequency impedancemetry, a non-invasive technique, to determine the deposition velocities of sand-water and biomass-water mixtures over a wide range of concentrations and pumped over a range of velocities much wider than the common industrial practice. It was proven suitable to be a replacement for traditional and invasive methods, being able to measure very low slurry deposition velocities.

The concept of transportation is simple; nevertheless, the proper design of the pipeline requires complex models. According to Leporini *et al.* (2018), several researchers tried and failed to develop a model to characterize slug transportation in pipelines accurately. Turian *et al.* (1987) performed a detailed examination of the critical velocity in pipeline flow on non-colloidal slurries. The authors reviewed 31 analytical literature correlations to predict the critical velocity, reorganized them into a standard form and compared with a collection of 864 data points of velocity data from the literature. The deviations range from 25 to 750%, with an average of 92%. The analytical description of the behavior of slurry pipeline transportation is made based on macroscopic experimental phenomena, which limits the real-time flow characteristics simulation and results in an incomplete description (Ting *et al.*, 2019).

Numerical simulation has become a useful research tool to describe the characteristics of slurry transportation, and it is receiving increasing attention. A simulation of polydispersed settling particles was performed by Capecelatro and Desjardins (2013). The authors used a high-fidelity large eddy simulation combined with a Lagrangian particle tracking solver to study a fully developed turbulent flow, in two cases: one operated above the critical deposition velocity and another below this limit. Most numerical studies apply the CFD-DEM coupling to describe the characteristics of slurry flow (Cleary, Hilton and Sinnott, 2017; Zhang, Gutierrez and Li, 2017; Zhang, Li and Gutierrez, 2017; Fatahi and Farzanegan, 2018; Uzi and Levy, 2018; Yang *et al.*, 2018; Zeng *et al.*, 2018). The computational fluid dynamics (CFD) is used to model the fluid motion by applying mass and momentum conservation equations, and the discrete element method (DEM) is used to model the motion of discrete particles by applying Newton`s laws of motion.

The CFD-DEM numerical approach was used to study laminar solid-liquid mixing in a stirred tank equipped with a pitched blade turbine (Blais *et al.*, 2016), to simulate the erosion of sediment particles submerged in water and mudflows at various shear flow velocities (Zheng *et al.*, 2018), to investigate the slurry infiltration and filter cake formation processes, simulating the slurry column test (Zhang and Yin, 2018; Zhang *et al.*, 2019), to study particle separation in a centrifugal separator (Ma *et al.*, 2019) and to analyze the characteristics of coarse particles in a pipeline under different velocities (Ting *et al.*, 2019).

This paper presents the assessment of the critical deposition velocity in slurries containing particles of apatite and hematite. Experimental results from the literature (Souza Pinto *et al.*, 2014) were used to validate numerical findings. For two recirculating pipeline test rigs, Souza Pinto *et al.* (2014) measured the pressure drop in a section 1 m long in a horizontal pipeline, for different pump speeds. In this work, the CFD-DEM was used to predict the characteristics of the flow, for five different velocities. The critical deposition velocity was determined and compared with literature data.

2. MATHEMATICAL MODEL

A CFD-DEM coupling simulation is used to investigate the mechanisms of particle-fluid flow interactions. Many research papers reviewed the CFD modeling (Patankar and Joseph, 2001; Agrawal *et al.*, 2018; Fullmer and Musser, 2018; Wang *et al.*, 2019); therefore, only a brief description is presented here. The simulation is based on three open-source codes: a CFD cope OpenFOAM (Open Source Field Operation and Manipulation), LIGGGHTS (LAMMPS Improved for General Granular and Granular Heat Transfer Simulations) and their coupled computation code CFDEM, used to determine the fluid-particle forces.

2.1 CFD Model

The mass and momentum conservation equations describe the liquid phase (Versteeg and Malaskekera, 1995):

$$\frac{\partial \rho}{\partial t} + \rho . \nabla u = 0 \tag{1}$$

$$\rho\left(\frac{\partial u}{\partial t} + u.\nabla u\right) = -\nabla p + \mu_{eq}\nabla^2 u + S \tag{2}$$

Where ρ is the fluid specific mass, t is time, u is the flow velocity, p is the pressure, μ_{eq} is the dynamic equivalent viscosity, and S is the source term.

The flow is assumed turbulent, and to this purpose, the k-ε turbulence model was used, as in Reyes and Ihle (2018). The transport equations for the turbulent properties k (turbulent kinetic energy) and ε (turbulent kinetic energy dissipation) are given by

$$\frac{\partial \rho k}{\partial t} + \frac{\partial \rho k u_i}{\partial x_i} = \frac{\partial}{\partial x_i}\left(\frac{\mu_t}{\sigma_k}\frac{\partial k}{\partial x_j}\right) + 2\mu_t E_{ij} E_{ij} - \rho\epsilon \tag{3}$$

$$\frac{\partial \rho \epsilon}{\partial t} + \frac{\partial \rho \epsilon u_i}{\partial x_i} = \frac{\partial}{\partial x_j}\left(\frac{\mu_t}{\sigma_\epsilon}\frac{\partial \epsilon}{\partial x_j}\right) + C_{1\epsilon}\frac{\epsilon}{k}2\mu_t E_{ij} E_{ij} - C_{2\epsilon}\rho\frac{\epsilon^2}{k} \tag{4}$$

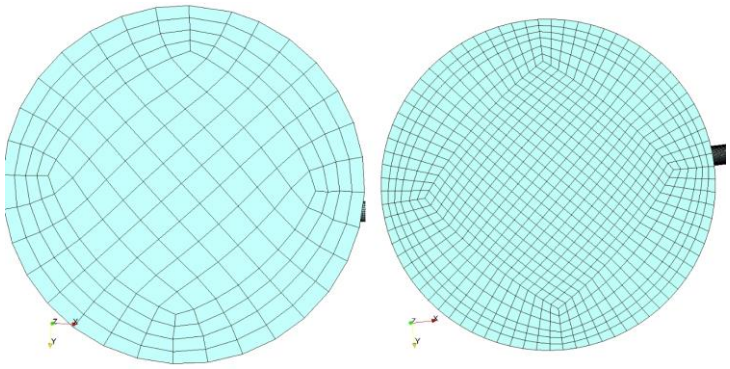

Fig. 1. CFD meshes used in the simulation.

The turbulent viscosity μ_t is

$$\mu_t = \rho C_\mu \frac{k^2}{\epsilon} \frac{\partial \rho k}{\partial t} + \frac{\partial \rho k u_i}{\partial x_i} = \frac{\partial}{\partial x_i}\left(\frac{\mu_t}{\sigma_k}\frac{\partial k}{\partial x_j}\right) + \\ +2\mu_t E_{ij} E_{ij} - \rho\epsilon \quad (5)$$

2.2 DEM Model

The solid phase is assumed to be a discrete phase and is described by the DEM method first proposed by (Cundall P and Strack D, 1979). The particle movement obeys Newton`s laws of motion. During its movement, the particle may collide with other particles or with walls, exchanging momentum (Kuang, Zhou and Yu, 2019). The contact forces depend on the characteristics of the materials of the particles. The assumptions used are:

- Each particle comprehend a complex system working along with other particles;
- Each particle has its independent motion and influences the motion of the neighbor particles;
- All the medium and all the particles are considered rigid bodies;
- The contact point between particles is infinitesimal;
- There is a tolerance for penetration between particles.

3. MATERIALS AND METHODS

This paper studies the critical deposition velocity of a mixture of water and apatite (12% in volume), inside two recirculating pipeline test rigs, with a pipe diameter of 50 mm. The granulometry of the particles varied from 249 to 297 micrometers. The geometry was based on literature data from

(Souza Pinto *et al.*, 2014). In this reference, pumping experiments were conducted, measuring the pressure drop in 1 m horizontal pipe. The authors determined the curve of pressure gradient versus bulk flow velocity. The solution domain is, therefore, based on the geometry of the experiments conducted by (Souza Pinto *et al.*, 2014). The solution domain represents part of the experimental setup, focusing on the region of the tube. It is 1.6 m high and 2.2 m of total length.

Four size meshes were used, starting from sparse (Mesh 1) to dense (Mesh 4), as shown in Fig. 1. The numbers of elements of the meshes are, respectively, 250560, 443700, 794952, and 1841856. An uncertainty analysis of the numerical errors of calculations in the computational analysis was performed for the entire domain, following (Roache, 2002). It was found that mesh 1 was able to take into account the computation time comprehensively and results accuracy, with suitable numerical uncertainties (below 3% in the entire domain).

The corresponding properties for the fluid and particles and boundary conditions were based on experimental data from (Souza Pinto *et al.*, 2014). The fluid is water at 15°C and the particles of apatite have a specific mass of 3120 kg/m3. The properties of the contact particle-tube were of PVC tube, with an elasticity module of 2.9 GPa.

For the walls, a no-slip condition was set. At the inlet, five different velocities were prescribed: 1.3 m/s, 1.8 m/s, 2.1 m/s, 2.4 m/s and 2.7 m/s. The first value is below the expected critical deposition velocity. At the outlet, fully developed conditions were specified, with zero relative pressure. The total length required for the flow to become fully developed is between 0.5 m and 3.0 m (corresponding to $10 < x/D < 60$). Although the total length is lower than 3.0 m, the fully developed condition is assumed to most pipe and duct flows in CFD analyzes (Autodesk, 2019). The computer used in the simulations was an Intel i7 processor of 3.4 GHz, 32 Gb of RAM (1600 MHz), 120 GB SSD and 3 Gb DDR5 video card.

4. RESULTS AND DISCUSSION

Five different velocities were prescribed as the inlet velocity in the tube. Souza Pinto *et al.* (Souza Pinto *et al.*, 2014) determined the critical deposition velocity as 1.8 m/s; therefore, the first value simulated was below the expected velocity. For each velocity, the suspension state of the particles was analyzed.

Figure 2 shows the velocity of the particles for the inlet fluid velocity of 1.3 m/s. The maximum velocity obtained was 2.5 m/s. The inlet region and the region after the elbow are shown in details. It can

be seen that the solid particles formed a stationary bed at the bottom of the horizontal section of the pipe, indicating that the critical deposition velocity was not reached.

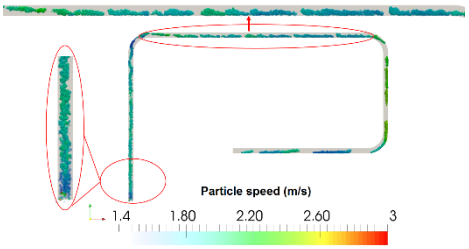

Fig. 2. Particles suspension state – 1.3m/s.

The transient behavior of the particles was evaluated on the horizontal section of the tube and is presented in Fig. 3, for the fluid velocity of 1.3 m/s. The amount of particles increases with time.

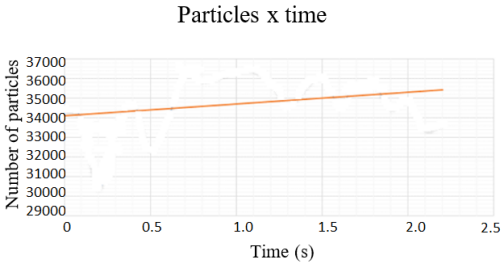

Fig. 3. Amount of particles x time– 1.3m/s.

The experimental value obtained for the critical deposition velocity was 1.8 m/s (Souza Pinto *et al.*, 2014). Nevertheless, numerical results indicated that, for this velocity, there is still a stationary bed formed at the bottom of the pipe (Fig. 4), showing that the critical velocity is higher than 1.8 m/s. For this condition, the maximum velocity of the particles was 2.7 m/s. Figure 5 shows the variation of the number of particles with time. The amount of particles is increasing. Nevertheless, the angular coefficient of the line is decreasing with the velocity.

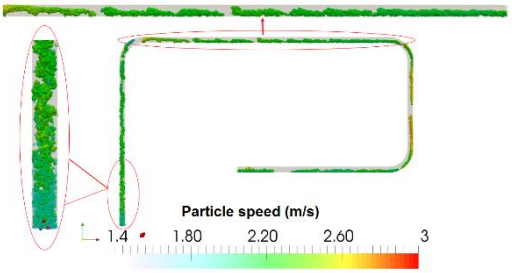

Fig. 4. Particles suspension state – 1.8m/s.

Figure 6 shows that, for the velocity of 2.1 m/s, there is still a bed formed at the bottom of the tube. However, as indicated in Fig. 7, although the angular coefficient still has a positive slope, the amount of particles is not increasing as much as observed for the lower velocities.

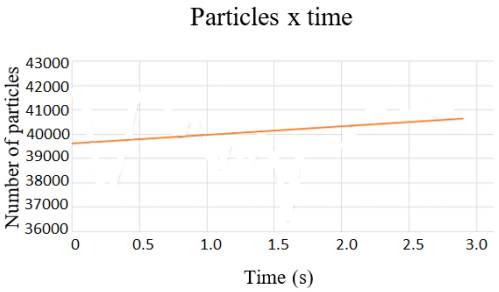

Fig. 5. Amount of particles x time – 1.8m/s.

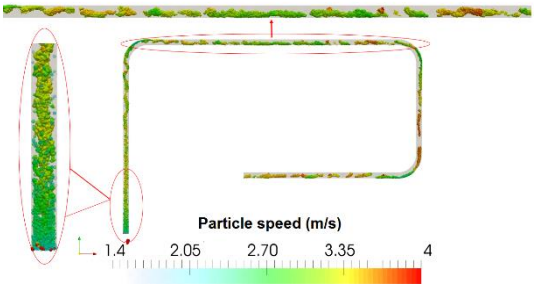

Fig. 6. Particles suspension state – 2.1m/s.

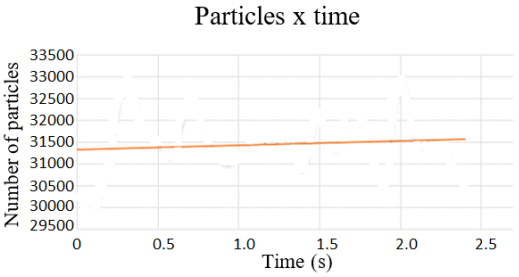

Fig. 7. Amount of particles x time – 2.1m/s.

Figures 8 and 9 show the behavior of the particles for the fluid velocity of 2.4 m/s. It can be seen a negative slope of the tendency line (Fig. 9), which means that the fluid flow removes the solid particles accumulated at the bottom of the pipe. Comparing the results found in Figs. 6 to 9, it can be inferred that the critical deposition velocity is between 2.1 m/s and 2.4 m/s, a difference of about 22% of experimental results from the literature (Souza Pinto *et al.*, 2014).

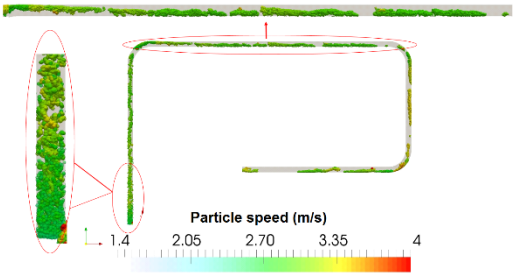

Fig. 8. Particles suspension state – 2.4m/s.

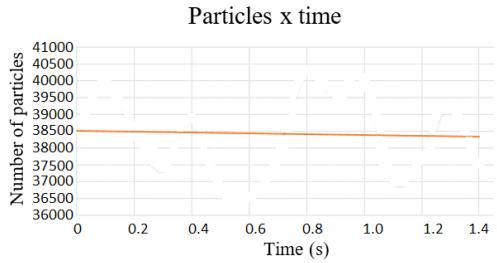

Fig. 9. Amount of particles x time – 2.4m/s.

Figures 10 and 11 show the behavior of the particles for the fluid velocity of 2.7 m/s. It can be seen that, for this velocity, there is no formation of the stationary bed at the bottom of the pipe and that the angular coefficient of the tendency line is also negative.

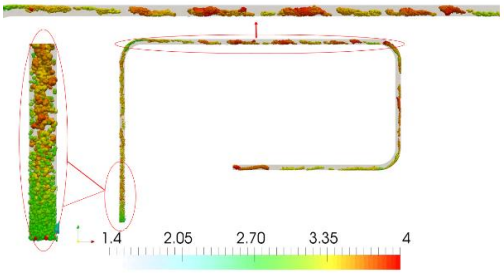

Fig. 10. Particles suspension state – 2.7m/s.

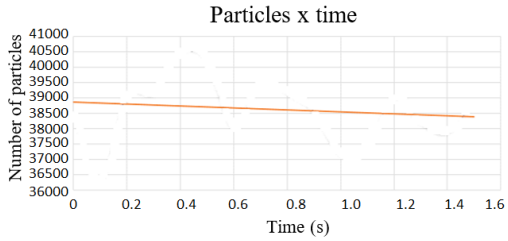

Fig. 11. Amount of particles x time – 2.7m/s.

Several parameters affect the critical deposition velocity, such as mineral concentration, particle size, pipe diameter, and pipe roughness. The results presented in this paper were obtained for the conditions defined by (Souza Pinto *et al.*, 2014), who performed the experimental analysis. Discrepancies found between the results obtained in this paper and the results from (Souza Pinto *et al.*, 2014) can be attributed to differences between experimental and estimated values and the lack of data. The pipe material used in the experiments was PVC, assumed as a smooth pipe, but the actual roughness of the pipe may affect the results. Simple assumptions for the boundary conditions are often made in numerical computations, due to the difficulty to acquire some inputs with a high degree of accuracy, as explained by (Versteeg and Malaskekera, 1995). It can affect the calculation results. Other numerical difficulties found during the simulation may deviate numerical results from the measured data. Also, as established by (Turian, Hsu and Ma, 1987), the accurate experimental estimation of the critical velocity in pipelines is a challenging task.

5. CONCLUSIONS

The CFD-DEM method was used in this study to analyze the characteristics of slurry flow under different velocities. The velocity of the fluid flow plays an important role in the deposition of particles at the bottom of the pipe. Below a critical value, there is a formation of a stationary bed at the bottom of the pipe, and there is a tendency for the particles to accumulate on the tube. Above this critical value, the fluid flow can remove the particles accumulated. The numerical determination of the critical deposition velocity of slurry is very important to the proper design of pipelines. The analysis can be performed to different concentrations of the solids, replacing experimental studies.

It was found a critical deposition velocity higher than the obtained by experimental data from the literature. It may be attributed to difficulties experimented during the numerical analysis, and also to the fact that the critical condition is difficult to discern, and consequently, to be determined experimentally.

ACKNOWLEDGMENTS

The authors would like to thank PUC Minas, FAPEMIG, and CNPq.

REFERENCES

Agrawal, V., Y. Shinde, M. T. Shah, R. P.Utikar, V. K. Pareek and J. B. Joshi (2018). Effect of drag models on CFD–DEM predictions of bubbling fluidized beds with Geldart D particles. *Advanced Powder Technology* 29(11), 2658-2669.

Autodesk (2019). *Flow boundary conditions - User guide*. Available at: https://knowledge.autodesk.com/support/cfd/learn-explore/caas/CloudHelp/cloudhelp/2014/ENU/SimCFD/files/GUID-9C1E28D5-B32E-4546-8620-7F428982184A-htm.html.

Bhabra, H. (2013). 'Slurry pipeline now goes the distance. *World Pumps*, 2013(6), 38-40.

Blais, B., M. Lassaigne, C. Goniva, L. Fradette, F. Bertrand (2016). Development of an unresolved CFD-DEM model for the flow of viscous suspensions and its application to solid-liquid mixing. *Journal of Computational Physics* 318, 201-221.

Capecelatro, J. and O. Desjardins (2013). Eulerian-Lagrangian modeling of turbulent liquid-solid slurries in horizontal pipes. *International Journal of Multiphase Flow* 55, 64–79.

CFDEM (no date) *CFDEM coupling Documentation, 2019*. Available at: https://www.cfdem.com/media/CFDEM/docu/CFDEMcoupling_Manual.html.

Cleary, P. W., J. E. Hilton and M. D. Sinnott (2017). Modelling of industrial particle and multiphase flows. *Powder Technology* 314, 232-252.

Cundall, P, A. and D. L.Strack (1979). A Discrete numerical model for granular assemblies. *Geotechnique* 29(1), 47-65.

Dabirian, R., R. Mohan, O. Shoham, G. Kouba (2016). Critical sand deposition velocity for gas-liquid stratified flow in horizontal pipes. *Journal of Natural Gas Science and Engineering*, 33, 527-537.

Fatahi, M. R. and A. Farzanegan (2018). An analysis of multiphase flow and solids separation inside Knelson Concentrator based on four-way coupling of CFD and DEM simulation methods. *Minerals Engineering*, 126, 130-144.

Fullmer, W. D. and J. Musser (2018). CFD-DEM solution verification: Fixed-bed studies. *Powder Technology* 339, 760-764.

Kuang, S., M. Zhou and A. Yu (2019). CFD-DEM modelling and simulation of pneumatic conveying: A review. *Powder Technology* 2-23.

Leporini, M., B. Marchetti, F. Corvaro, G. di Giovine, F. Polonara, A. Terenzi (2018). 'Sand transport in multiphase flow mixtures in a horizontal pipeline: An experimental investigation. *Petroleum*.

Ma, L., L. Wei, X. Pei, X. Zhu, D. Xu (2019). CFD-DEM simulations of particle separation characteristic in centrifugal compounding force field. *Powder Technology* 343, 11-18.

Patankar, N. A. and D. D. Joseph (2001). Modeling and numerical simulation of particulate flows by the Eulerian-Lagrangian approach. *International Journal of Multiphase Flow* 27(10), 1659-1684.

Reyes, C. and C. F. Ihle (2018). Numerical simulation of cation exchange in fine-coarse seawater slurry pipeline flow. *Minerals Engineering* 117 14-23.

Roache, P. J. (2002). Quantification 9f Uncertainty in Computational Fluid Dynamics. *Annual Review of Fluid*

Souza Pinto, T. C., D. Moraes Junior, P. T. Slatter, L. S. Leal Filho (2014). Modelling the critical velocity for heterogeneous flow of mineral slurries. *International Journal of Multiphase Flow* 65, 31-37.

Ting, X. *et al.* (2019). Study of the characteristics of the flow regimes and dynamics of coarse particles in pipeline transportation. *Powder Technology*. 347, 148-158.

Turian, R. M., F. L. Hsu and T. W. Ma (1987). Estimation of the critical velocity in pipeline flow of slurries. *Powder Technology* 51(1), 35-47.

Uzi, A. and A. Levy (2018). Flow characteristics of coarse particles in horizontal hydraulic conveying. *Powder Technology* 326, 302-321.

Vaezi, M., S. Verma and A. Kumar (2018). Application of high-frequency impedancemetry approach in measuring the deposition velocities of biomass and sand slurry flows in pipelines. *Chemical Engineering Research and Design* 140, 142-154.

Versteeg, H. K. and W. Malaskekera (1995) *An Introduction to Computational Fluid Dynamics: The Finite Volume Method*, *Fluid flow handbook.* McGraw-Hill.

Wang, S., K. Luo, C. Hu, J. Lin, J. Fan (2019). CFD-DEM simulation of heat transfer in fluidized beds: Model verification, validation, and application. *Chemical Engineering Science* 197, 280-295.

Yang, D., Y. Xia, D. Wu, P. Chen, G. Zeng, X. Zhao (2018). Numerical investigation of pipeline transport characteristics of slurry shield under gravel stratum. *Tunnelling and Underground Space Technology* 71, 223-230.

Zeng, D., E. Zhang, Y. Ding, Y. Yi, Q. Xian, G. Yao, H. Zhu, T. Shi (2018). Investigation of erosion behaviors of sulfur-particle-laden gas flow in an elbow via a CFD-DEM coupling method. *Powder Technology* 329, 115–128.

Zhang, G., M. Gutierrez and M. Li (2017). A coupled CFD-DEM approach to model particle-fluid mixture transport between two parallel plates to improve understanding of proppant micromechanics in hydraulic fractures. *Powder Technology* 308, 235-248.

Zhang, G., Li, M. and M. Gutierrez (2017). Simulation of the transport and placement of multi-sized proppant in hydraulic fractures using a coupled CFD-DEM approach. *Advanced Powder Technology* 28(7), 1704-1718.

Zhang, Z., T. Yin, X. Huang, D. Dias (2019). Slurry filtration process and filter cake formation during shield tunnelling: Insight from coupled CFD-DEM simulations of slurry filtration column test. *Tunnelling and Underground Space Technology*. Elsevier, 87(December 2018), pp. 64–77.

Zhang, Z. and T. Yin (2018). A Coupled CFD–DEM Simulation of Slurry Infiltration and Filter Cake Formation during Slurry Shield Tunneling. *Infrastructures* 3(2), 15.

Zheng, H. C. *et al.* (2018). Coupled CFD-DEM model for the direct numerical simulation of sediment bed erosion by viscous shear flow', *Engineering Geology* 245, 309-321.

Zorgani, E., H. Al-Awadi, W. Yan, S. Al-lababid, H. Yeung, C. P. Fairhurst (2018). Viscosity effects on sand flow regimes and transport velocity in horizontal pipelines. *Experimental Thermal and Fluid Science* 89-96.

APPENDIX 1 – EXPERIMENTAL SETUP

The geometry used in this paper was based on literature data from (Souza Pinto *et al.*, 2014). In this reference, pumping experiments were conducted with slurries containing coarse particles of different minerals. The experimental set-up consists of two recirculating pipeline test rigs with transparent sections (Fig. 12). A U-shaped manometer, inverted

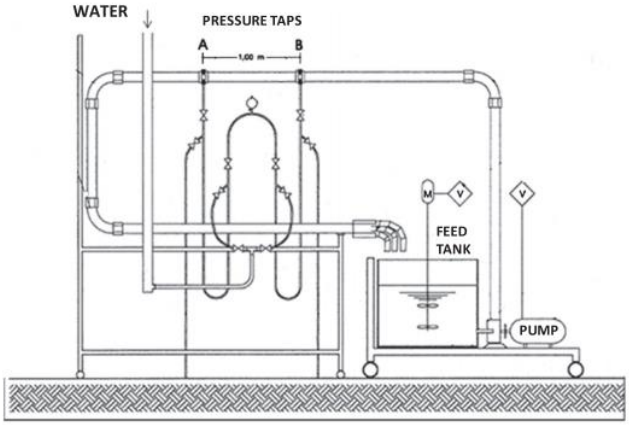

Fig. 12. Schematics of the experimental setup used for validation.

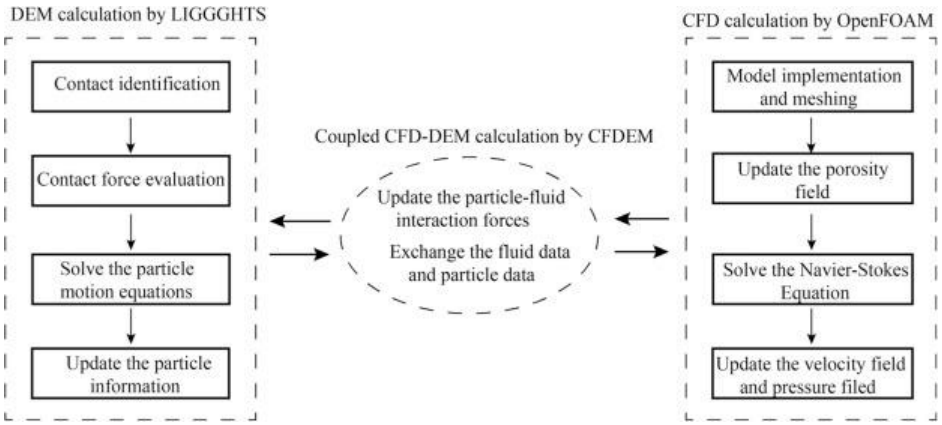

Fig. 13. Overview of the CFD-DEM simulation.

and filled with air, using water as the working fluid, was used to measure the pressure drop along the pipe. A feed tank was filled with a defined volume of water to adjust the concentration of the slurry. The U-shaped manometer was then filled with water. The solids were added to the feed tank, and the mixture was homogenized. The pump speed was varied with a variable frequency, and the pressure drop was measured in 1 m horizontal pipe.

APPENDIX 2 – CFD-DEM SOFTWARE

In this work, it was performed a numerical analysis using a coupled CFD-DEM simulation, based on the open source codes OpenFOAM, LIGGGHTS and CFDEM. This section describes the details of the codes.

OpenFOAM is a C++ toolbox for the development of numerical solvers. The solver applications have a syntax that closely resembles the partial differential equations being solved. The fluid motion is described using the mass and momentum conservation equations, solved by OpenFOAM packages. The fluid and particles interact with each other, creating fluid-particle interaction forces. To take into account the effect of these forces on the fluid it is necessary to define a solid fraction and a solid field velocity, both given by the DEM simulations.

LIGGGHTS is an open source software, improved from the classical simulator Lammps to be applied in industrial applications. It is a simulation code for conducting Discrete Element Method particle simulation software.The velocity and position of the particles are described based on the integration of Newton's second law. The translational (vi) and rotational (wi) motion of a particle is given by (Blais *et al.*, 2016)

$$m_i \frac{dv_i}{dt} = \sum_j f_{c,ij} + \sum_k f_{lr,ik} + f_{pf,i} + f_{g,i}$$

$$I_i \frac{d\omega_i}{dt} = \sum_j \left(M_{t,ij} + M_{r,ij}\right)$$

For a particle I, m is the mass, I is the moment of inertia, fc, flr, ppf and fg are the contact, long-range (non-contact), particle-fluid interaction and body forces, respectively. Mt and Mr are the tangential and rolling friction moments.

Figure 13 describes the major procedures of a coupled CFD-DEM simulation (Zhang *et al.*, 2019).

The CFD-DEM coupling combines LIGGGHTS and OpenFoam free source codes. It solves the Navier-Stokes equations with a solid phase. The general formulation is given by (CFDEM, no date):

$$\frac{\partial(\alpha_l \rho_l)}{\partial t} + \nabla \cdot (\alpha_l \rho_l u_l) = 0$$

$$\frac{\partial(\alpha_l \rho_l u_l)}{\partial t} + \nabla \cdot (\alpha_l \rho_l u_l u_l) = -\alpha_l \nabla p + \\ -K_{sl}(u_l - u_s) + \nabla \cdot (\alpha_l \tau) + \alpha_l \rho_l g + f$$

In the previous equations, l and s refer to liquid and solid. α is the liquid sontent of a cell, ρ is the density, u is the velocity, p is the pressure, τ is the tension, g is the gravity and K is the implicit momentum exchange between liquid and solid phases. F is a general term that can be used to explicitly exchange momentum between liquid and solid phases.

Development of an unresolved CFD–DEM model for the flow of viscous suspensions and its application to solid–liquid mixing